

- 7) Hikita, H., K. Ishimi and H. Ikeki: *J. Chem. Eng. Japan*, **10**, 375 (1977).  
 8) Hikita, H., K. Ishimi, Y. Omotehara and T. Fukase: *J. Chem. Eng. Japan*, **11**, 96 (1978).  
 9) Jackson, M. L. and N. H. Ceaglske: *Ind. Eng. Chem.*, **42**, 1188 (1950).  
 10) McCarter, R. J. and L. F. Stutzman: *AIChE J.*, **5**, 502 (1959).  
 11) Reker, J. R., C. A. Plank and E. R. Gerhard: *AIChE J.*, **12**, 1008 (1966).  
 12) Yoshida, T. and T. Hyodo: *Ind. Eng. Chem., Process Des. Develop.*, **9**, 207 (1970).

## CHARACTERISTIC FLOW BEHAVIOR OF HIGH SWIRLING JET IN A CIRCULAR VESSEL

CHIAKI KURODA AND KOHEI OGAWA

*Department of Chemical Engineering, Tokyo Institute of Technology, Tokyo 152*

**Key Words:** Fluid Mechanics, Swirling Jet, Swirl Reynolds Number, Reynolds Number, Reverse Flow, Swirl Intensity

A swirling jet has been put to practical use to control hot air flow in spray driers, flames in combustors, etc. by using characteristic flow behavior such as reverse flow. If the intensity of swirl is weak, the flow behavior is relatively simple and its structure can be estimated by appropriate operational parameters, e.g. the Swirl number  $Sw$ .<sup>1,5)</sup> However, the three-dimensional flow behavior becomes more complicated as the intensity of swirl increases and reverse flow appears. Hence, the investigation of a high swirling jet with reverse flow is considered necessary.

In this study, a high swirling turbulent jet in a circular vessel is taken up and the characteristic axial flow behavior is mainly investigated by measuring three-dimensional velocity components of water flow with an electrochemical technique.

### 1. Experimental Apparatus and Procedure

The experimental apparatus consists of two vertical acrylic-resin coaxial circular pipes with inside diameters  $D_1$  ( $=100$  mm) and  $D_2$  ( $=290$  mm). The test fluid in the smaller pipe spouts into the larger one as jet flow. In the smaller pipe the test fluid is supplied through two entrances. One is an axial entrance and the other is a tangential entrance. The flow rates are denoted by  $Q_z$  and  $Q_\theta$  respectively and the total flow rate  $Q$  is represented by the sum of  $Q_z$  and  $Q_\theta$ . The tangential entrance consists of two inlet pipes with an inside diameter  $d$  ( $=10$  mm), which are attached tangentially to the smaller test pipe. An axial stream and a tangential stream join and spour into the larger

pipe 0.5 m downstream from the tangential entrance as a swirling jet.

Three-dimensional measurements of velocity were performed by using an electrochemical multi-electrode probe<sup>3)</sup> in downstream cross sections 0.1 m and 0.3 m from the jet exit. In almost the same measuring range, some visualization experiments of flow were performed by using polystyrene particles with a diameter of about 1.2 mm.

In this study, two kinds of dimensionless operational parameters, i.e., the general Reynolds number  $Re$  and the swirl Reynolds number  $Re_\theta$ , which were proposed in the previous paper,<sup>4)</sup> are used.  $Re$  is based on the cross-sectional average velocity  $U_a$  in the small pipe as follows:

$$\begin{aligned} Re &= D_1 U_a / \nu \\ &= 2Q / (\pi \nu R_1) \end{aligned} \quad (1)$$

$Re_\theta$  is based on the characteristic angular velocity  $\omega_i$  at the jet exit. To determine the value of  $\omega_i$ , the idea of the intensity of swirl  $\Gamma$  (the circulation) which was proposed in the previous paper<sup>2)</sup> on swirling pipe flow is used. The value of  $\Gamma$  at the jet exit, i.e.,  $\Gamma_i$  ( $=2\pi R_1^2 \omega_{i1} = 2\pi R_2^2 \omega_{i2}$ ), can be calculated from the initial condition at the tangential entrance by using the experimental equation<sup>2)</sup> of the decay process of  $\Gamma$  in the small pipe as follows:

$$\begin{aligned} \Gamma_i / (2\pi R_1^2 \omega_0) \\ = 0.26 \exp\{-7100(0.5/R_1)(\nu/(R_1^2 \omega_0))\} \end{aligned} \quad (2)$$

$$\omega_0 = 2Q_\theta / (\pi d^2 R_1) \quad (3)$$

Received May 20, 1986. Correspondence concerning this article should be addressed to C. Kuroda.

As a result,  $Re_\theta$  is expressed as follows:

$$Re_\theta = R_1^2 \omega_{i1} / \nu$$

$$= \Gamma_i / (2\pi\nu) \quad (4)$$

The experiments were conducted at  $Re$  of 2400–14300 and  $Re_\theta$  of 0–76200.

If the mean tangential velocity and the mean axial velocity are assumed to be  $\bar{U}_\theta = \omega_{i1}r$  and  $\bar{U}_z = U_a$  at the jet exit of the small pipe, the Swirl number  $Sw^{1,5)}$  can be expressed by  $Re$  and  $Re_\theta$  as follows by neglecting the pressure term:

$$Sw = Re_\theta / Re \quad (5)$$

The above  $Sw$  is used as an approximate reference value of the Swirl number.

## 2. Results and Discussion

### 2.1 Visual experiments

Figure 1 shows photographs of vertical sections containing the center axis when polystyrene particles are injected into swirling jets at  $Re = 14300$  and  $Re_\theta =$  variable. Swirling jets expand in the radial direction more rapidly with increasing  $Re_\theta$ . Three types of axial flow behavior were observed as shown in Fig. 1 from trajectories of particles. The flow behavior changes from Type 1 to Type 2 and further to Type 3 with increasing  $Re_\theta$ . A reverse flow which goes upstream is a feature of Type 2, and the flow behavior of Type 3 is characterized by the property that the flow which goes downstream appears in the central reverse flow region.

### 2.2 Axial mean velocity and three types of axial flow behavior

Some examples of distributions of the axial mean velocity component  $\bar{U}_z$  and the tangential mean velocity component  $\bar{U}_\theta$  at  $z = 0.1$  m are shown in Figs. 2 and 3, where negative  $\bar{U}_z$  shows reverse flow. As mentioned in Section 2.1, three types of axial flow behavior appear according to operational conditions, i.e.,  $Re$  and  $Re_\theta$ . Similar distributions are obtained also at  $z = 0.3$  m, and such flow types seem to be kept downstream to some extent. These three types of axial flow behavior are classified by operational conditions as shown in Fig. 4 for the case of  $D_2/D_1 = 2.9$ . This classification in Fig. 4 is based on both results of visual experiments and measurements of velocity in the region near the jet exit ( $z = 0.1-0.3$  m). In this figure, double keys mean the transitional flow behavior between two types. It seems that the flow behavior of Type 3 is apt to appear in very high swirling condition as shown in Figs. 3 and 4. The well-known criterion<sup>1,5)</sup> between Type 1 and Type 2, i.e.,  $Sw = 0.6$ , is indicated by a dotted line which is calculated from Eq. (5), and the criterion is almost satisfied in this study. The flow behavior changes from Type 2

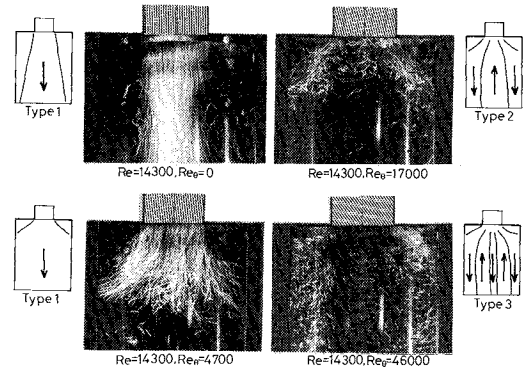


Fig. 1. Visualization of flow by use of polystyrene particles.

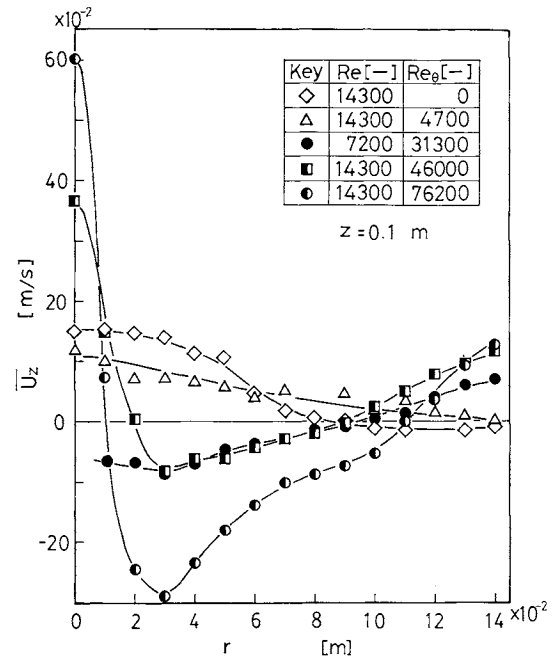


Fig. 2. Examples of distributions of axial mean velocity.

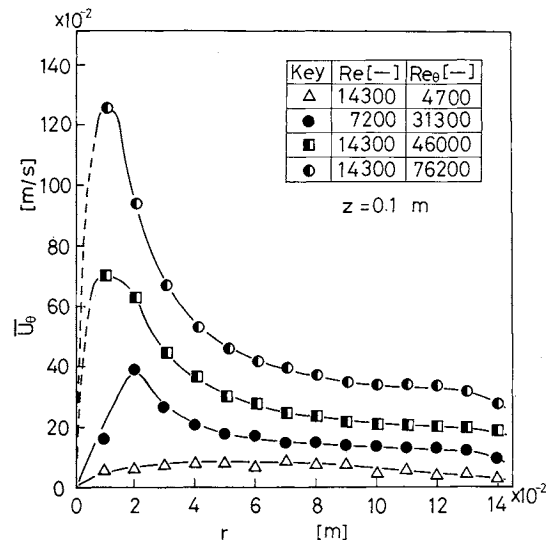


Fig. 3. Examples of distributions of tangential mean velocity.

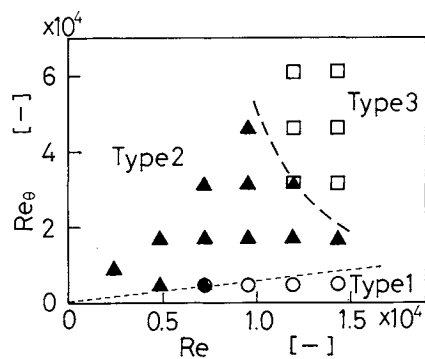


Fig. 4. Three types of axial flow behavior and operational conditions ( $D_2/D_1 = 2.9$ ).

to Type 3 with increasing  $Re$  and  $Re_\theta$ , and it is difficult to make clear the criterion between Type 2 and Type 3 by using only  $Sw$ . That criterion is approximately expressed by the following equation within the present experimental conditions:

$$Re \cdot Re_\theta^{0.4} = 7.5 \times 10^5 \quad (6)$$

#### Nomenclature

$D$	= inner diameter of pipe	[m]
$d$	= inner diameter of tangential inlet pipe	[m]
$Q$	= flow rate	[m <sup>3</sup> /s]
$R$	= inner radius of pipe	[m]
$Re$	= general Reynolds number, Eq. (1)	[—]

$Re_\theta$	= swirl Reynolds number, Eq. (4)	[—]
$r$	= radius	[m]
$Sw$	= Swirl number	[—]
$\bar{U}$	= time-mean velocity	[m/s]
$U_a$	= cross-sectional average velocity in jet nozzle pipe (small pipe)	[m/s]
$z$	= axial distance from jet exit	[m]
$\Gamma$	= intensity of swirl over cross section	[m <sup>2</sup> /s]
$\Gamma_i$	= intensity of swirl at jet exit	[m <sup>2</sup> /s]
$\nu$	= kinematic viscosity	[m <sup>2</sup> /s]
$\omega_i$	= characteristic angular velocity at jet exit	[1/s]
$\omega_0$	= characteristic angular velocity at tangential entrance	[1/s]

#### <Subscripts>

1	= jet nozzle pipe (small pipe)
2	= test vessel (large pipe)
$r, \theta, z$	= radial, tangential and axial direction

#### Literature Cited

- 1) Gupta, A. K., D. G. Lilley and N. Syred: "Swirl Flows," Abacus Press (1984).
- 2) Ito, S., K. Ogawa and C. Kuroda: *Kagaku Kogaku Ronbunshu*, **4**, 247 (1978).
- 3) Ito, S., S. Urushiyama and K. Ogawa: *J. Chem. Eng. Japan*, **7**, 462 (1974).
- 4) Kuroda, C., K. Ogawa and I. Inoue: *J. Chem. Eng. Japan*, **18**, 439 (1985).
- 5) Syred, N. and J. M. Beer: *Combustion and Flame*, **23**, 143 (1974).

## THE CONTROLLING QUANTITY IN CUBIC EQUATION OF STATE FOR HEAT OF VAPORIZATION CALCULATIONS

YOSHINORI ADACHI AND HIDEZUMI SUGIE

Center of Information Processing Education, Nagoya Institute of Technology, Nagoya 466

**Key Words:** Phase Equilibrium, Thermodynamics, Enthalpy Vaporization, Cubic Equation, Cohesion Parameter

### Introduction

This study concerns the calculation of heat of vaporization,  $H^{\text{vap}}$ , by means of a cubic equation of state (EoS). Its purpose is to show that the same  $\Omega_a$  EoSs (EoSs which have the same cohesion parameter  $\Omega_a$ ) give identical  $H^{\text{vap}}$  results and to show that the ability of an EoS to predict  $PVT$  properties is not related to the  $H^{\text{vap}}$  calculation.

### 1. Cubic Equations of State

The following general cubic EoS is considered:

$$P = \frac{RT}{V-b_1} - \frac{a}{(V-b_2)(V-b_3)} \quad (1)$$

where "a",  $b_1$ ,  $b_2$  and  $b_3$  are constants, and  $a = \Omega_a R^2 T_c^2 / P_c$  is the only quantity considered to be temperature-dependent. At the critical point, Eq. (1) satisfies the critical constraints:

Received May 26, 1986. Correspondence concerning this article should be addressed to Y. Adachi.